nature immunology

CD1d-lipid antigen recognition by the γδ TCR

Adam P Uldrich[1,5], Jérôme Le Nours[2,3,5], Daniel G Pellicci[1], Nicholas A Gherardin[1], Kirsty G McPherson[1], Ricky T Lim[1], Onisha Patel[2], Travis Beddoe[2], Stephanie Gras[2], Jamie Rossjohn[2–4,6] & Dale I Godfrey[1,6]

The T cell repertoire comprises αβ and γδ T cell lineages. Although it is established how αβ T cell antigen receptors (TCRs) interact with antigen presented by antigen-presenting molecules, this is unknown for γδ TCRs. We describe a population of human $V_\delta1^+$ γδ T cells that exhibit autoreactivity to CD1d and provide a molecular basis for how a γδ TCR binds CD1d–α-galactosylceramide (α-GalCer). The γδ TCR docked orthogonally, over the A′ pocket of CD1d, in which the $V_\delta1$-chain, and in particular the germ line–encoded CDR1δ loop, dominated interactions with CD1d. The TCR γ-chain sat peripherally to the interface, with the CDR3γ loop representing the principal determinant for α-GalCer specificity. Accordingly, we provide insight into how a γδ TCR binds specifically to a lipid-loaded antigen-presenting molecule.

The αβ T cell antigen receptor (TCR) can recognize antigenic peptides, lipids and microbial metabolites presented by major histocompatibility complex (MHC) molecules, CD1 family molecules and MR1 molecules, respectively, thereby enabling a broad survey of self and foreign antigens encountered by the host[1–3]. Despite the discovery of the γδ T cell lineage more than 25 years ago[4], the type of antigens targeted by γδ TCRs and the importance of antigen presentation in γδ TCR recognition, is much less clear[5]. Several studies have shown that γδ TCRs can recognize MHC or MHC-like molecules in an antigen-independent manner. For example, some mouse γδ T cells recognize MHC class II molecules regardless of the type of bound peptide antigen[6]. Others recognize the inducible T10 and T22 molecules, ligands which adopt an atypical MHC-like fold and do not present antigen[7,8]. Under conditions of cellular stress, some human γδ T cells can bind to the MHC class I–like endothelial protein C receptor (EPCR) in a ligand-independent manner[9]. Conversely, populations of γδ T cells exist that seemingly recognize antigens, including phosphoantigens[10], in the absence of antigen-presenting molecules. However, a recent study showed that $V_\gamma9V_\delta2$ T cells are activated by phosphorylated prenyl metabolites when presented by butyrophilin BTN3A1 (ref. 11). Some γδ T cells recognize lipid-based antigens presented by CD1 family members. For example, human $V_\delta1^+$ γδ T cells can recognize phospholipid antigens presented by CD1a, CD1c or CD1d[12,13], and a recent study demonstrated γδ TCR recognition of the mammalian glycolipid antigen, sulfatide, when presented by CD1d[14].

The recognition of lipid antigens presented by CD1d is usually associated with natural killer T (NKT) cells, which are subdivided into type I and type II subsets[3]. Type I NKT cells express an αβ TCR consisting of an invariant TCR α-chain ($V_\alpha24$-$J_\alpha18$ in humans) paired with a limited array of TCR β-chains. The prototypical ligand for type I NKT cells is α-galactosylceramide (α-GalCer)[3], although other ligands, including microbial lipids, mammalian β-linked glycolipids and phospholipids, can activate type I NKT cells[15]. Type II NKT cells, although CD1d-restricted, neither express the invariant type I NKT TCR α-chain nor recognize α-GalCer. Nevertheless, type II NKT cells can express a diverse TCR repertoire and respond to a range of lipid antigens, including sulfatide[3]. Consistent with these observations, the mode of recognition of CD1d-antigen by type I and type II NKT TCRs can be fundamentally different[16,17]. However, the molecular basis for recognition of CD1–lipid antigen complexes by γδ T cells is unknown. Moreover, the structural basis for antigen recognition by γδ T cells remains unclear. The structures of some unliganded γδ TCRs, or domains thereof, have been determined[18–20]. However, only one γδ TCR co-complex structure has been published, namely the structure of a complex of γδ TCR with the nonclassical MHC molecule T22, in which a lengthy and autonomous CDR3δ loop protruded into the empty cleft of the T22 molecule[21,22].

Here we identified and characterized a diverse population of human $V_\delta1^+$ γδ T cells that exhibit CD1d autoreactivity, yet this recognition can be modulated by bound lipid antigen, including α-GalCer. We provide a molecular basis of how a $V_\delta1^+$ γδ TCR interacts with CD1d bound to α-GalCer, revealing that the germ line–encoded CDR1δ loop underpinned CD1d restriction whereas the CDR3γ loop determined antigen specificity. Accordingly, we provide insight into how a γδ TCR binds to a ligand presented by an antigen-presenting molecule.

RESULTS

Identification of CD1d–α-GalCer tetramer-reactive γδ T cells

We identified a population of CD1d–α-GalCer tetramer$^+$ cells in human peripheral blood that express γδ TCRs (**Fig. 1a**). These cells showed lower CD1d–α-GalCer tetramer staining than type I

[1]Department of Microbiology and Immunology, Peter Doherty Institute for Infection and Immunity, University of Melbourne, Parkville, Victoria, Australia. [2]Department of Biochemistry and Molecular Biology, School of Biomedical Sciences, Monash University, Clayton, Victoria, Australia. [3]Australian Research Council Centre of Excellence in Structural and Functional Microbial Genomics, Monash University, Clayton, Victoria, Australia. [4]Institute of Infection and Immunity, Cardiff University, School of Medicine, Heath Park, Cardiff, UK. [5]These authors contributed equally to this work. [6]These authors jointly directed this work. Correspondence should be addressed to J.R. (jamie.rossjohn@monash.edu) or D.I.G. (godfrey@unimelb.edu.au).

Received 17 May; accepted 20 August; published online 29 September 2013; doi:10.1038/ni.2713

NKT cells and were typically less frequent, although in one donor they were of a similar frequency. Next we enriched CD1d–α-GalCer tetramer$^+$ cells from peripheral blood mononuclear cells (PBMCs) and expanded these cells in culture for 2 weeks *in vitro*. We detected a clear population of γδ TCR$^+$ cells representing 0.05–3.5% of CD1d–α-GalCer tetramer$^+$ cells in 11 of 21 different NKT cell–enriched samples from healthy individuals (three of which are represented in **Fig. 1b**). Human CD1d 'unloaded' tetramer, which contains endogenous lipid antigen, also stained these γδ T cells in most cases, indicating CD1d autoreactivity. Human γδ T cells were not labeled with mouse CD1d–α-GalCer tetramer nor with mouse CD1d 'unloaded' tetramer, whereas human type I NKT cells were

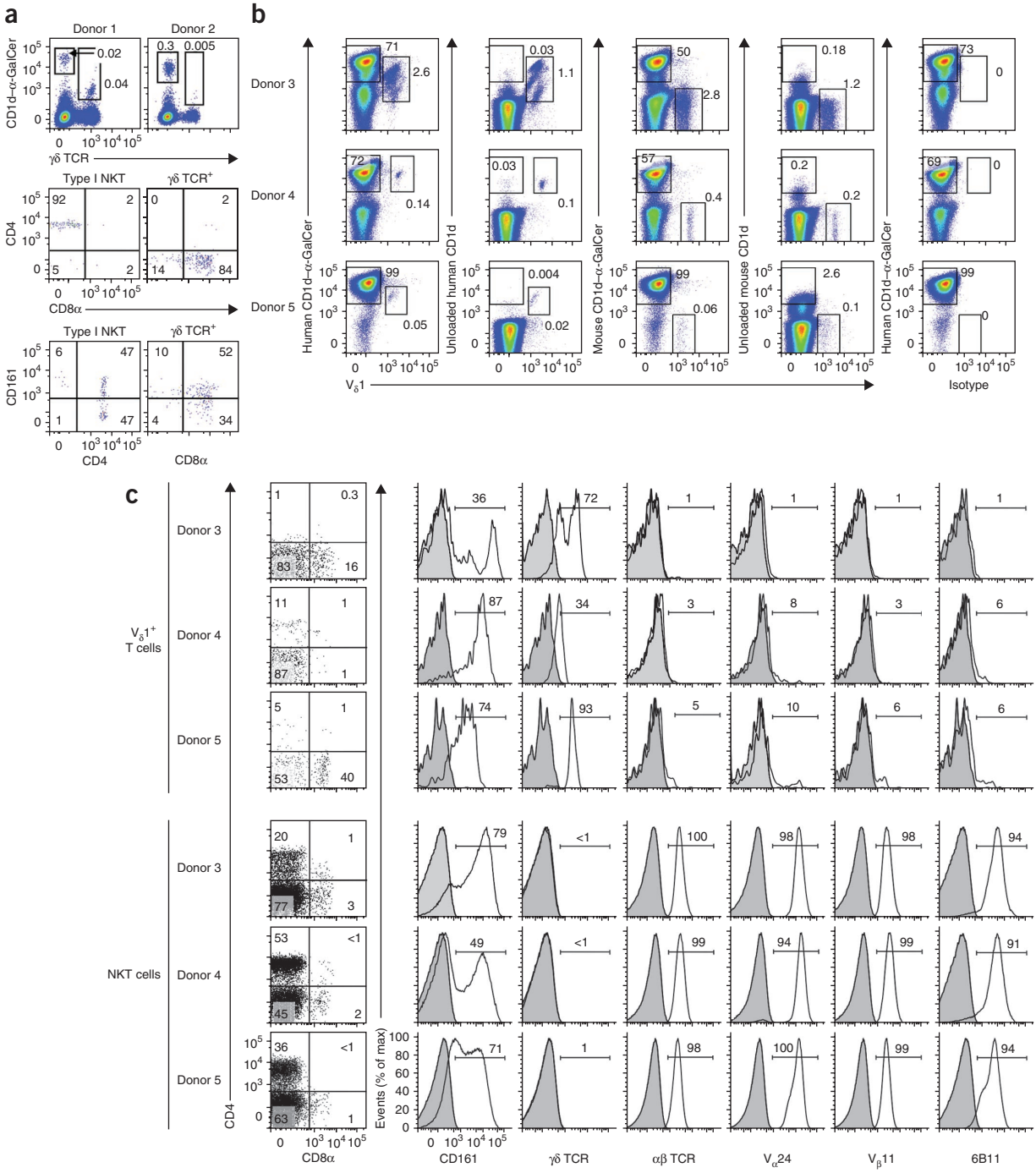

Figure 1 Identification of $V_\delta1^+$ cells reactive to CD1d–α-GalCer. (**a**) Flow cytometry analysis of healthy human PBMCs from two donors showing γδ TCR and human CD1d–α-GalCer tetramer staining on gated CD3$^+$ cells (top), and CD4, CD8 and CD161 staining on CD3$^+$ CD1d–α-GalCer tetramer$^+$ γδ TCR$^+$ cells or CD3$^+$ CD1d–α-GalCer tetramer$^+$ γδ TCR$^-$ (type I NKT) from donor 1 (middle and bottom). (**b**) Flow cytometry analysis showing $V_\delta1$ versus mouse and human CD1d tetramer (loaded with α-GalCer or 'unloaded') staining on CD3$^+$ cells from *in vitro*–expanded CD1d–α-GalCer tetramer–enriched PBMCs from three donors. (**c**) Expression of CD161, γδ TCR, αβ TCR, $V_\alpha24$, $V_\beta11$ and $V_\alpha24$-$J_\alpha18$ (clone 6B11) on CD3$^+$ $V_\delta1^+$ CD1d–α-GalCer tetramer$^+$ ($V_\delta1^+$ T cells) and CD3$^+$ $V_\delta1^-$ CD1d–α-GalCer tetramer$^+$ (NKT cells) prepared from three donors as in **b**. Data shown represent 5 separate donors, performed over two experiments. Numbers in plots indicate percent of gated events.

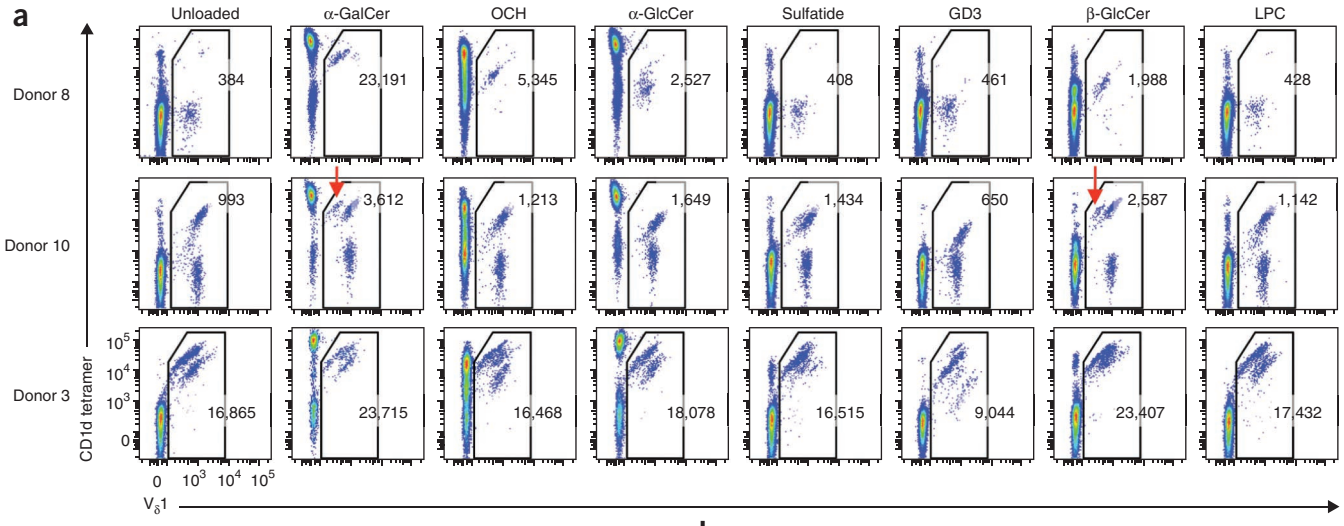

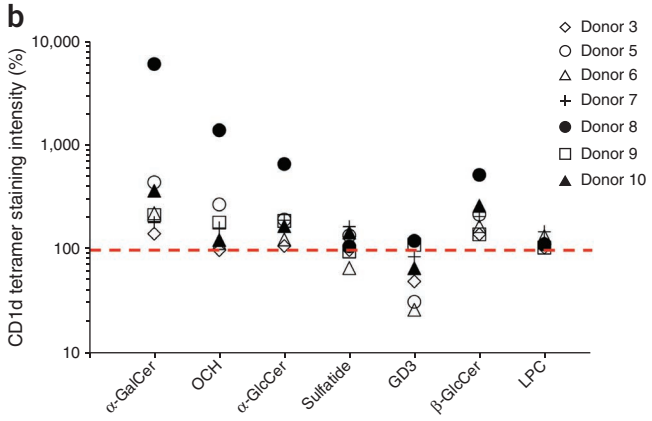

Figure 2 Lipid antigen reactivity of autoreactive CD1d-restricted γδ T cells. (**a**) Flow cytometry analysis of *in vitro*–expanded CD1d–α-GalCer tetramer-enriched PBMCs from three donors, showing human CD1d tetramer staining loaded with different glycolipid antigens, or unloaded, as indicated. The geometric mean fluorescence intensity (arbitrary units) for the cells in each region is shown for each plot. Red arrows indicate a subset of CD1d-lipid–reactive $V_\delta1^+$ cells. (**b**) Binding of CD1d–lipid tetramers normalized against 'unloaded' CD1d tetramer (indicated by the dashed red line). Data are representative of two experiments. OCH, α-GalCer analog OCH.

strongly cross-reactive with the mouse reagents. This highlighted a clear difference in the reactivity of the γδ T cells and the type I NKT cells. CD1d–α-GalCer tetramer$^+$ γδ T cells were predominantly $V_\delta1^+$ (**Fig. 1b**); $V_\delta1$ is typically expressed by tissue-homing γδ T cells and is underrepresented in blood γδ T cells[5]. In contrast to type I NKT cells, many of which were CD4$^+$, the CD1d–α-GalCer tetramer$^+$ γδ T cells were predominantly CD4$^-$CD8$^-$ or CD8$^+$ and CD161$^+$ (**Fig. 1a**,**c**), did not express $V_\alpha24$ or $V_\beta11$ and were not stained with the 6B11 antibody specific for the invariant $J_\alpha18$-encoded CDR3α loop of human type I NKT cells (**Fig. 1c**). Thus, $V_\delta1^+$ γδ T cells represent a subset of CD1d–α-GalCer–reactive T cells in human blood that are distinct from type I NKT cells in their cell-surface phenotype, their ability to bind to human CD1d in the absence of α-GalCer and their lack of cross-reactivity to mouse CD1d–α-GalCer.

Lipid-antigen recognition by CD1d-restricted γδ T cells

To examine the influence of lipid antigens on the γδ TCR–CD1d interaction, we loaded a panel of antigens into human CD1d tetramers and tested them against *in vitro*–expanded CD1d–α-GalCer tetramer$^+$ γδ T cells (**Fig. 2** and data not shown). In some donors (for example, donor 8), the presence of α-GalCer strongly increased the tetramer staining intensity over CD1d 'unloaded' tetramer; in others (for example, donor 3), there was little difference; whereas other donors (for example, donor 10) had a subset of γδ T cells that was stained more brightly with CD1d–α-GalCer tetramer compared to CD1d 'unloaded' tetramer and another subset that was stained to a similar degree by both tetramers (**Fig. 2a**). We also observed different staining intensity of the CD1d–α-GalCer tetramer$^+$ γδ T cells with other glycolipid antigens (**Fig. 2a**). For example, the γδ T cells from donor 8 were strongly stained with CD1d–α-GalCer tetramer yet were much less reactive to CD1d–α-glucosylceramide (α-GlcCer) tetramer and CD1d–β-GlcCer tetramer. A subset of CD1d–α-GalCer tetramer$^+$ cells from donor 10 showed a similar high staining with CD1d–α-GalCer tetramer and CD1d–β-GlcCer tetramer yet much weaker staining with CD1d–α-GlcCer tetramer. In most cases, there was little change in staining intensity with CD1d tetramers loaded with the self-glycolipid sulfatide and the phospholipids lysophosphatidylcholine (LPC) (**Fig. 2**) and LPE (data not shown) compared to CD1d 'unloaded' tetramers. In contrast, in many cases, CD1d-GD3 (a tumor-associated ganglioside) tetramers showed lower staining intensity compared to CD1d 'unloaded' tetramers, indicating that some lipid antigens can inhibit CD1d recognition. Thus, although we observed staining with CD1d 'unloaded' tetramers on $V_\delta1^+$ cells from most donors, this 'autoreactivity' can be modulated in a glycolipid antigen–dependent and donor-dependent manner. This suggests that CD1d-restricted γδ TCRs recognize both CD1d and the associated lipid antigens. Moreover, in contrast to αβ TCR$^+$ NKT cells, which tend to be quite similar in their reactivity between donors, there was considerable interdonor variability in the pattern of antigen recognition by the CD1d-restricted $V_\delta1^+$ population.

The cytokine profile of CD1d–α-GalCer tetramer$^+$ γδ T cells

Type I NKT cells produce high amounts of a broad range of cytokines within hours of stimulation. To investigate whether the CD1d–α-GalCer tetramer$^+$ γδ T cells had similar functional potential, we sorted γδ T cells from short-term cultured CD1d–α-GalCer tetramer–enriched cell cultures from four separate donors, stimulated them *in vitro* with the phorbol ester PMA plus ionomycin for 20 h and tested them for various cytokines using a cytometric bead array

Table 1 CD1d–α-GalCer–restricted γδ TCR sequences

		TCRδ		TCRγ	
Sequence	Donor	V_δ-D_δ-J_δ	CDR3δ	V_γ-J_γ	CDR3γ
1	3	$V_\delta1$-$D_\delta3$-$J_\delta1$	CALGELGGVPGDRELIF	$V_\gamma8$-J_γP2	CATWPPYSSDWIKTF
2	3	$V_\delta1$-$D_\delta3$-$J_\delta1$	CALGVWGDKLIF	$V_\gamma5$-$J_\gamma1$	CATWDRLYYKKLF
3	3	$V_\delta1$-$J_\delta2$	CALGELLVRSSLTAQLFF	$V_\gamma2$-$J_\gamma1$	CATWDGLSYKKLF
4	3	$V_\delta1$-$D_\delta2$-$D_\delta3$-$J_\delta1$	CALGGSLVGDLNTDKLIF	ND	
5	4	$V_\delta1$-$D_\delta3$-$J_\delta1$	CALGDPGGLNTDKLIF	$V_\gamma5$-$J_\gamma1$	CATWDRGNPKTHYYKKLF
6	5	$V_\delta1$-$D_\delta3$-$J_\delta1$	CALGELWGFPNRDKLIF	$V_\gamma9$-$J_\gamma1$	CALWEARPFYYKKLF
7	6	$V_\delta1$-$D_\delta2$-$D_\delta3$-$J_\delta1$	CALGEPFLRSLIWEYTDKLIF	$V_\gamma5$-$J_\gamma2$	CATWDRPEANYYKKLF
8	6	$V_\delta1$-$D_\delta2$-$D_\delta3$-$J_\delta1$	CALGETFLPSLGGWTDKLIF	$V_\gamma5$-$J_\gamma1$	CATWDALAKLF

	CDR1	**CDR2**
$V_\delta1$	TSWWSYY	QGS
$V_\alpha24$	VS**PFS**N	MTFSENT

Paired TCR sequences from single cell–sorted CD3$^+$ CD1d–α-GalCer tetramer$^+$ $V_\delta1^+$ cells isolated from CD1d–α-GalCer tetramer-enriched and *in vitro*–expanded PBMCs (top). ND, not determined. Sequences of CDR1 and CDR2 regions of $V_\delta1$ and $V_\alpha24$ with residues involved in type I NKT TCR recognition of α-GalCer shown in bold (bottom).

(**Supplementary Fig. 1**). Type I NKT cells, which we used as a control, produced high amounts of IFN-γ, tumor necrosis factor, granulocyte macrophage colony-stimulating factor, and interleukins IL-4, IL-5 and IL-13. We detected a similar range of cytokines in the purified CD1d–α-GalCer tetramer$^+$ γδ T cell cultures, although γδ T cells generally produced less of these cytokines compared to type I NKT cells from each separate donor and showed considerable variation from donor to donor. We did not detect IL-17A in any cultures (data not shown). Thus, γδ T cells appear to be similar to type I NKT cells in their diversity of cytokine production.

CD1d-restricted γδ TCR reactivity

Next, using flow cytometry, we sorted individual cells and used single-cell sequencing of cDNA to determine TCR gene rearrangements encoding paired TCR γ-chain and TCR δ-chain proteins. We derived paired TCR gene sequences from 18 of 24 separate cells from four donors, of which seven were unique (**Table 1**). These sequences supported the common use of $V_\delta1$ by these γδ T cells, rearranged with an array of D_δ and J_δ genes, paired with a TCR γ-chain consisting of various V_γ and J_γ genes. We selected one of these γδ TCR pairs for subsequent analysis (clone 9C2, TCR $V_\gamma5$-$V_\delta1^+$; sequence number 5 from donor 4) because the γδ T cells in this donor showed stronger reactivity to CD1d–α-GalCer in comparison to CD1d 'unloaded' tetramer (**Fig. 1b**). We transduced a Jurkat-76 cell line with a vector encoding this 9C2 γδ TCR (here referred to as 'Jurkat.9C2'). We loaded human CD1d tetramers with a selection of lipid antigens and used them to stain TCR vector–transduced cell lines expressing either the 9C2 γδ TCR, a type I NKT TCR, or an irrelevant control peptide-MHC–specific TCR (**Fig. 3a**). The irrelevant peptide-MHC–specific TCR did not support any CD1d tetramer staining. Type I NKT cells were stained by CD1d tetramers loaded with each of these lipids at a higher level than CD1d 'unloaded' tetramer, and as expected, these were not sulfatide-reactive. Consistent with the data from *in vitro*–expanded cells, the 9C2 γδ TCR conferred autoreactivity to CD1d 'unloaded' tetramers, and staining was clearly enhanced with CD1d–α-GalCer. However, most of the other glycolipid antigens caused little, if any, enhanced CD1d tetramer staining, apart from sulfatide, which resulted in a moderate increase in staining intensity. Given that the main distinction between α-GalCer and the other antigens is the nature of the glycosyl head group, these data suggest that the 9C2 γδ TCR recognizes both CD1d and α-GalCer.

To determine whether antigen recognition by these CD1d tetramer$^+$ γδ TCRs could activate T cells, we cocultured Jurkat.9C2 cells with C1R cells that expressed human CD1d at either intermediate or high abundance. The Jurkat.9C2 cells upregulated CD69 expression after 6–12 h of coculture, and upregulation correlated with the amount of CD1d expressed by the C1R cells (**Fig. 3b**). CD1d$^-$ parental C1R cells did not induce upregulation of CD69, similar to Jurkat.9C2 cells cultured in the absence of C1R cells. An irrelevant peptide-MHC–specific TCR$^+$ Jurkat cell line showed no induction of CD69 in response to any of the C1R cells (**Fig. 3b**). Therefore, the 9C2 γδ TCR reflects the CD1d autoreactivity observed for the original γδ T cells from donor 4. Next, we examined $V_\delta1^+$ CD1d–α-GalCer tetramer$^+$ cells derived from short-term cultures from six different donors for activation after culture with CD1d^{hi} C1R cells. We observed CD69 upregulation in at least three of six of these cultures, and this was enhanced by the presence of α-GalCer (**Fig. 3c**). Type I NKT cells in the same cultures were also activated by CD1d^{hi} C1R cells but only in the presence of α-GalCer (**Fig. 3c**). Taken together, these data confirm that the γδ TCRs expressed by these CD1d tetramer$^+$ γδ T cells can bind to CD1d and can result in activation of T cells, and that this interaction can be modulated by different lipid antigens.

γδ TCR–CD1d-antigen binding affinity

Next we undertook molecular and structural studies of the 9C2 TCR, as CD1d recognition by this γδ TCR was dependent on the nature of the glycolipid antigen bound (**Fig. 3a**). We expressed soluble, correctly folded, 9C2 γδ TCR in mammalian cells and subsequently removed the leucine zippers and His tags by thrombin cleavage (**Supplementary Fig. 2a–c**). We used surface plasmon resonance (SPR) to determine the affinity of the interaction between the 9C2 γδ TCR and CD1d–α-GalCer, and compare this to the affinity of a typical human type I NKT TCR interaction with CD1d–α-GalCer[23] (**Fig. 3d**). The γδ TCR bound CD1d–α-GalCer with good affinity (dissociation constant (K_d) = 16 μM), albeit not as high as the affinity type I NKT TCR exhibited for CD1d–α-GalCer (K_d = 0.5 μM). Consistent with the binding of CD1d 'unloaded' tetramer, the 9C2 γδ TCR also bound to CD1d 'unloaded', albeit with lower affinity (K_d = 35 μM), whereas the type I NKT TCR did not bind (**Fig. 3d**). These data support the concept that although the 9C2 γδ TCR exhibits some autoreactivity against CD1d self antigen, the presence of the agonist α-GalCer enhances the affinity of this interaction. This indicated that the 9C2 γδ TCR can interact with both the α-GalCer lipid antigen and the CD1d molecule.

9C2 γδ TCR structure

We initially solved the structure of the 9C2 γδ TCR in the unligated state (**Fig. 4** and **Supplementary Table 1**). The electron density corresponding to the unligated 9C2 γδ TCR was mostly unambiguous (data not shown), although residues 104–110 (sequence GNPKTHY) of the CDR3γ loop were unresolved, and we considered them to be flexible. The 9C2 γδ TCR adopted a similar structure to the previously determined γδ TCRs[18–20] (root mean square (r.m.s.) deviation of 0.9–1.7 Å on the variable (V)γ domain and 0.6–1.3 Å on the Vδ domain), which was distinct from the type I NKT TCR structure (**Fig. 4a**). The 9C2 γδ TCR did not have a lengthy hypervariable CDR3δ loop as observed in the G8 γδ TCR complexed to the nonclassical MHC, T22 (ref. 21). The 9C2 γδ TCR did not have a central electropositive cavity as had been observed in the unligated type I NKT TCR antigen-combining site[24] (**Fig. 4b**). However, the 9C2 γδ TCR comprised several

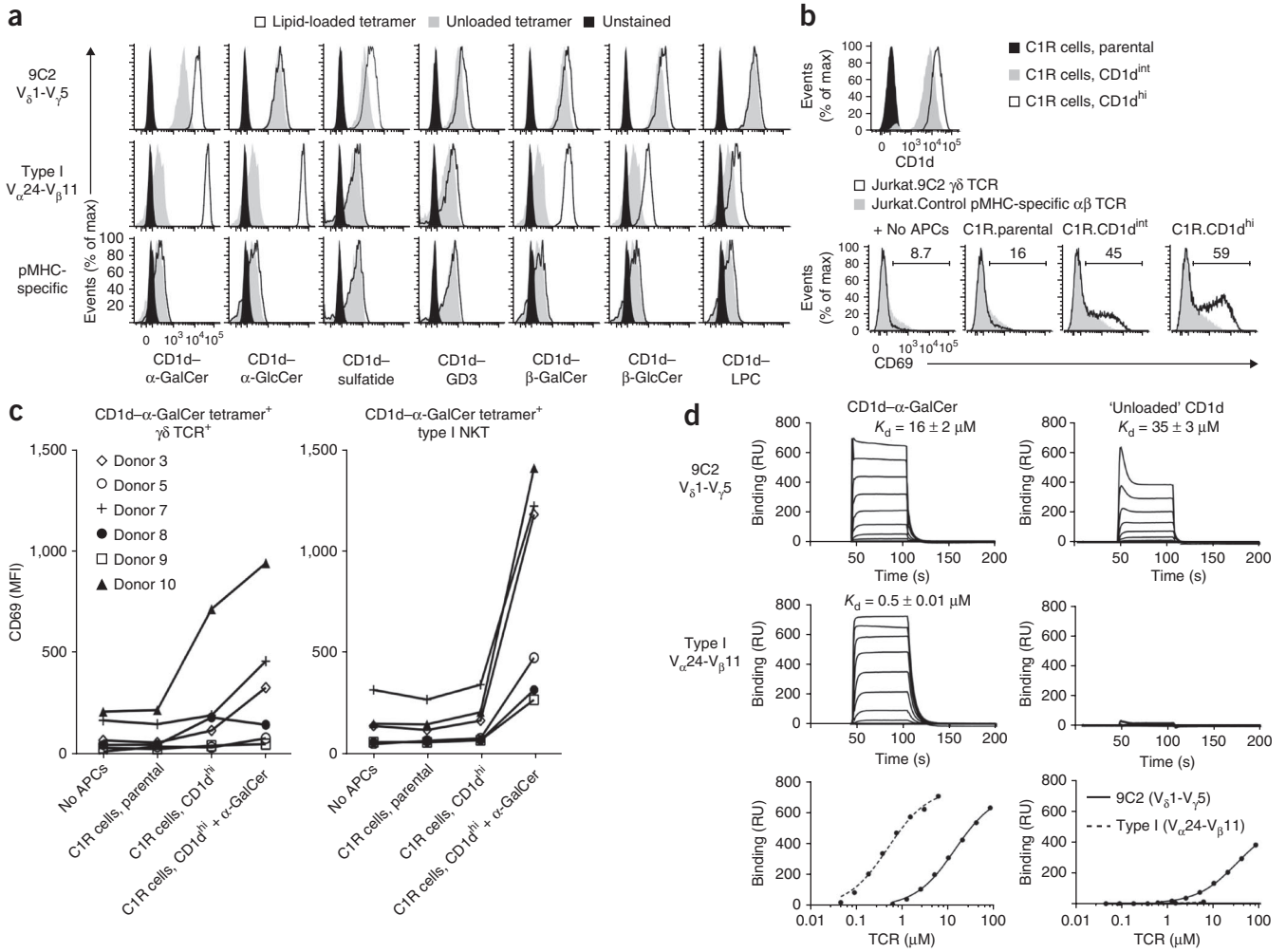

Figure 3 9C2 γδ–TCR reacts with CD1d–α-GalCer. (**a**) Flow cytometry analysis of cell lines expressing 9C2 γδ TCR, type I NKT αβ TCR or irrelevant peptide-MHC–specific αβ TCR, showing human CD1d tetramer staining loaded with various lipid antigens (white), unloaded CD1d tetramer (gray) and unstained cells (black) on electronically gated cells with equivalent amounts of surface CD3. Data are representative of two independent experiments. (**b**) Flow cytometry analysis of CD1d expression on C1R cells expressing intermediate or high amounts of CD1d (top), and CD69 expression on 9C2 γδ TCR or control pMHC-specific TCR-transduced Jurkat-76 (Jurkat) cells co-cultured with antigen-presenting cells (APCs) from indicated cells (bottom). Numbers in plots indicate percent of gated events. Data are representative of two independent experiments for all samples except data for 9C2 cultured alone or with C1R cells expressing $CD1d^{int}$ and $CD1d^{hi}$, which are representative of three independent experiments. (**c**) CD69 mean fluorescence intensity (MFI; arbitrary units) of gated $V_\delta1^+$ γδ TCR^+ CD1d–α-GalCer $tetramer^+$ cells (left) and $V_\delta1^-$ CD1d–α-GalCer $tetramer^+$ cells ('type I NKT', right), derived from *in vitro*–expanded CD1d–α-GalCer tetramer-enriched PBMCs that were cocultured with C1R parental or C1R $CD1d^{hi}$ APCs with or without α-GalCer for 6 h. Data represent 6 separate donors, screened in one experiment. (**d**) Binding affinity measured by surface plasmon resonance of 9C2 γδ TCR (top sensorgrams, 80 μM to 0.62 μM), type I NKT αβ TCR (middle sensorgrams, 6 μM to 0.047 μM) and saturation plots (bottom) for interaction of 9C2 γδ TCR and type I NKT αβ TCR with CD1d–α-GalCer (left) or 'unloaded' CD1d (right). RU, response units. Data shown are from one of two separate experiments, and K_d values represent the mean ± s.e.m. from two experiments.

surface-exposed aromatic residues in the complementarity determining regions (CDRs), including Phe34, Tyr35 and Tyr52 from the γ-chain and Trp32, Trp33 and Tyr36 from the $V_\delta1$ chain (**Fig. 4b**). Given the repeated selection of the $V_\delta1$ chain in the CD1d-restricted γδ T cells, this revealed a potentially important role for these bulky aromatic residues in enabling CD1d restriction.

Overview of the 9C2 γδ TCR–CD1d–α-GalCer complex

Next, we determined the structure of the 9C2 γδ TCR–CD1d–α-GalCer ternary complex (**Supplementary Table 1** and **Supplementary Fig. 3**). The γδ TCR docked orthogonally (87°) over the extreme end of the A′ pocket of CD1d (**Fig. 5a** and **Supplementary Table 2**). In contrast, all type I NKT TCRs dock in a parallel manner (20°; **Fig. 5c**,**f**) over the F′ pocket of CD1d, regardless of the identity of the antigen bound in the CD1d cleft[3]. As such, there were essentially no common CD1d interacting residues underpinning the γδ TCR and type I NKT TCR footprints, with the center of gravity between these two TCRs atop CD1d being approximately 28 Å and 41 Å apart for the V_δ-V_α and V_γ-V_β domains, respectively (**Supplementary Fig. 4**). The mode of γδ TCR–CD1d recognition was more reminiscent of how a recently described mouse type II NKT TCR (XV19) docked onto CD1d-sulfatide or CD1d-lysosulfatide[16,17] (**Fig. 5b**). The XV19 TCR sat above the A′ pocket of CD1d in an orthogonal docking mode (100°; **Fig. 5e**), although the γδ TCR was located even further toward the extreme pole of the A′ pocket (**Fig. 5d**). Moreover, whereas the α- and β-chains of the XV19 TCR were positioned centrally over the A′ pocket of CD1d, the TCR δ-chain was located above the helical jaws of CD1d, with the TCR γ-chain positioned peripherally to the

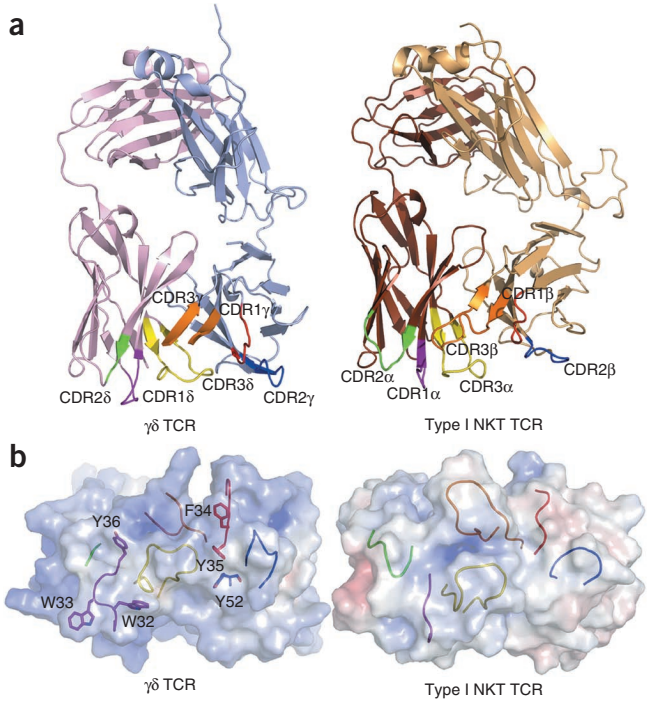

Figure 4 γδ TCR and type I NKT TCR structures. (**a**) Overview of the structures of the type I NKT (Protein Data Bank code 2PO6) and γδ TCRs. CDR1α and CDR1δ, purple; CDR2α and δ, green; CDR3α and δ, yellow; CDR1β and γ, red; CDR2β and γ, blue; and CDR3β and γ, orange. (**b**) Calculated molecular electrostatic surface potential of type I NKT and γδ TCRs. The location of the residues Phe34γ, Tyr35γ, Tyr52γ, Trp32δ, Trp33δ and Tyr36δ are indicated in the γδ TCR. Negative surfaces are in red, neutral surfaces in white and positive surfaces in blue.

α1-helix of CD1d. Indeed, the center of gravity between the respective γ/β-chains and δ/α-chains of the XV19 αβ TCR and the 9C2 γδ TCR were 7 Å and 10 Å apart, respectively. Thus, the γδ TCR docked onto CD1d-antigen in a distinct manner compared to type I and type II NKT TCR–CD1d recognition (**Fig. 5**), thereby highlighting the diverse mechanism by which the αβ TCR and γδ TCR lineages can interact with CD1d-antigen.

γδ TCR–CD1d interactions

The γδ TCR sat over CD1d such that TCR contacted residues spanning positions 58–69 and 152–171 of the α1-helix and the α2-helix of CD1d, respectively, with a buried surface area of ~950 Å^2 upon ligation, which compares to buried surface area of ~800 Å^2 and ~1,000 Å^2 for type I and type II NKT TCR-CD1d recognition, respectively (**Fig. 5g–i**). The 9C2 TCR γ-chain and TCR δ-chain contributed disproportionally upon engaging CD1d–α-GalCer, with the δ-chain dominating contacts (75% of the buried surface area) in comparison to the γ-chain (25% of the buried surface area; **Fig. 5g**). Namely, the CDR1δ and CDR3δ loops contributed 41% and 26% buried surface area, respectively, whereas only the CDR3γ loop of the γ-chain appreciably interacted with CD1d–α-GalCer (18% buried surface area; **Fig. 5g**). Accordingly, the germ line–encoded CDR1δ and non–germ line–encoded CDR3δ loop dominated the interactions at the 9C2 TCR-CD1d interface (**Fig. 5g**). These features contrast those of type I and type II NKT αβ TCR–CD1d-antigen interactions (**Fig. 5e**,**f**,**h**,**i**). In human type I NKT TCR–CD1d–α-GalCer recognition, the NKT TCR interacts with CD1d above the F′ pocket (residues 76–87 and 149–153), where the invariant α-chain contributes 66% of the buried surface area upon complexation, with the TCR β-chain interactions essentially being restricted to the CDR2β loop interacting with CD1d (**Fig. 5i**)[25]. In the case of autoreactive type I NKT TCRs, the hypervariable CDR3β loop mediates CD1d binding in an antigen-independent manner[26–28]. Regarding recognition of type II NKT TCR (**Fig. 5h**), the site of CD1d recognition (residues 65–72 and 154–167 of CD1d) overlapped with that of γδ TCR recognition (**Fig. 5g**)[16,17]. However, in contrast to γδ TCR binding, the α-chain and β-chain of the XV19 TCR contributed equally to CD1d-sulfatide binding, with the CDR3α and CDR3β loops dominating interactions at the interface (30% and 29% buried surface area, respectively)[17].

The majority of the 9C2 γδ TCR–CD1d contacts were hydrophobic, in which clusters of aromatic residues, arising from both the γδ TCR and CD1d itself, featured prominently. Although the CDR1γ loop was positioned above the α1-helix of CD1d, only Tyr35γ of the CDR1γ loop contacted CD1d, via a hydrogen bond with His68 (data not shown). Similarly, the CDR2γ loop sat peripheral to the α1-helix and did not contact CD1d, despite the presence of two germ line–encoded tyrosine residues, Tyr52γ and Tyr53γ, flanking and in the CDR2γ loop, respectively (data not shown). Further, the short CDR2δ loop (amino acids QGS at positions 54–56) had a marginal role in the interaction, with the abutting framework residue, Asp57 of the TCR δ-chain interacting primarily with a N-glycan moiety attached to Asn163 of CD1d (**Supplementary Table 2**). The CDR3δ loop had a key role in mediating contacts with CD1d, with this loop adopting an extended hairpin-like conformation, stretching across the antigen-binding cleft of CD1d, interacting with residues arising from the α1-helix and α2-helix, albeit with a greater extent of contacts with the α1-helix of CD1d (**Figs. 5a**,**d** and **6a**). Pro99 of the CDR3δ loop (Pro99δ) packed against Trp160, whereas Leu102δ was wedged between Thr65 and Ile69 of CD1d. Asn103δ and Thr104δ from the ascending region of the CDR3δ loop formed van der Waals contacts with His68 of CD1d, whereas Asp105δ contacted Thr65 of CD1d, and Lys106δ hydrogen-bonded to Gln61 (**Fig. 6a**). Notably, although the γ-chain had a very limited role in mediating contacts with CD1d, a cluster of aromatic residues appeared to have a critical role in maintaining the conformation of the CDR3δ loop. Namely, Phe34, Tyr35, His37, Tyr39, Tyr52 and Trp101 of the TCR γ-chain clustered around the CDR3δ loop (**Fig. 6b**), suggesting that a role of the γ-chain in enabling CD1d recognition is to ensure the structural integrity of the CDR3δ loop.

The CDR1δ loop had the major role in interacting with CD1d, by abutting the extreme end of the A′ pocket of CD1d and interacting with the both the α1-helix and α2-helix of CD1d. Ser31 of the CDR1δ loop hydrogen-bonded to Gln62 of CD1d, whereas Ser34δ contacted Trp160 and Gly164 of CD1d (**Fig. 6c**). Tyr36δ pointed toward CD1d, with its hydroxyl group contacting Glu156 (**Fig. 6c**). The CDR1δ-CD1d interaction site was dominated by three tryptophan residues: Trp32 and Trp33 of the CDR1δ loop from the 9C2 γδ TCR and Trp160 from CD1d. Trp32δ interdigitated between the helical jaws of the CD1d antigen-binding cleft, plugging a hydrophobic pocket that is lined by Gln62, Thr65 and Leu66 from the α1-helix, Phe58 from the cleft floor, and Trp160 and Thr165 from the α2-helix (**Fig. 6c**). Trp33δ abuts the α2-helix of CD1d, packing against its helical backbone as well as the aliphatic side chain of Gln168 and Pro167 (**Fig. 6c**). Trp160 of CD1d wedged between and formed backbone-mediated contacts with the CDR1δ and CDR3δ loops, as well as stacking against Trp32δ and Pro99δ. Accordingly, the tryptophan-rich germ-line–encoded CDR1δ loop has a major role in enabling this CD1d-restricted γδ TCR response.

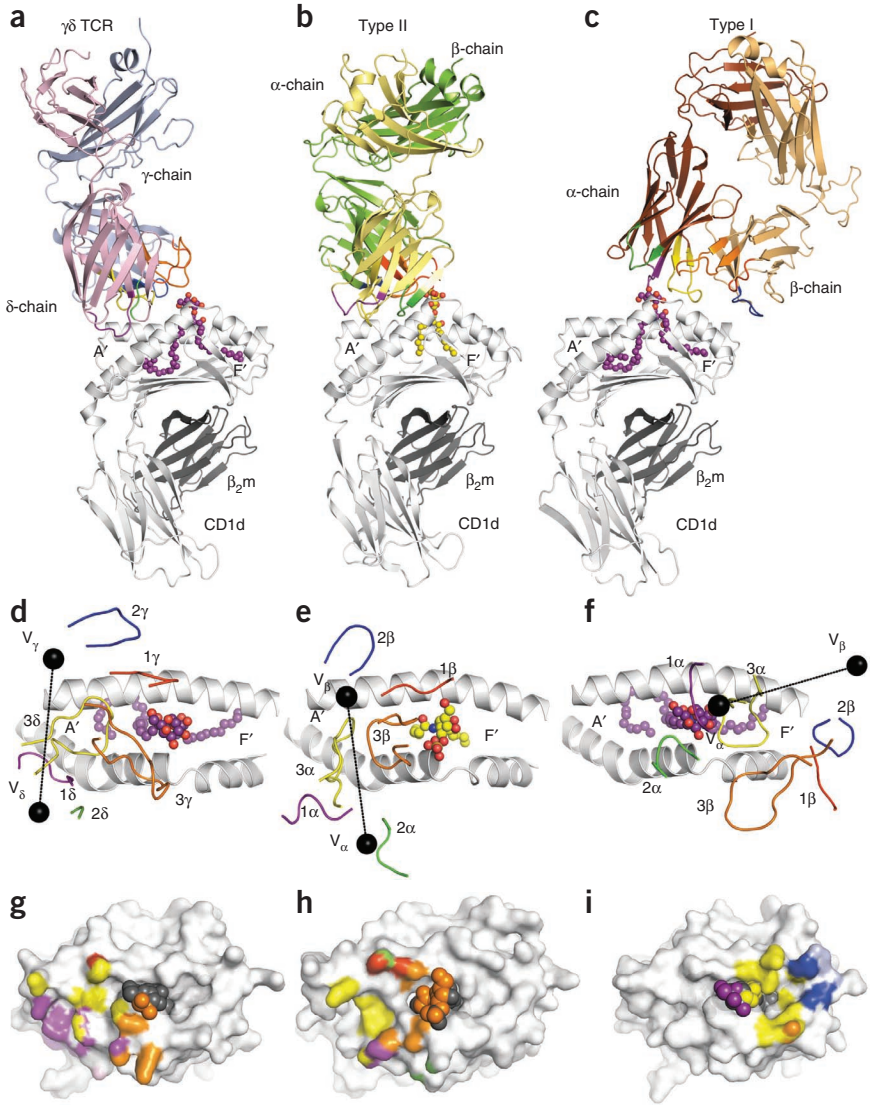

Figure 5 Overview of the CD1d-antigen complex with the γδ TCR. (**a**) CD1d–α-GalCer–γδ TCR ternary complex (pale pink and blue for the TCR δ- and γ-chains, and purple spheres for α-GalCer). (**b**) Mouse type II NKT cell TCR bound to CD1d–sulfatide (pale yellow and green for the TCR α- and β-chains, and yellow spheres for sulfatide; PDB code 4EI5). (**c**) Human type I NKT cell TCR bound to CD1d–α-GalCer (brown for the TCR α- and β-chains, and purple spheres for α-GalCer; PDB code 2P06). CD1d molecules are depicted in white, β_2 microglobulin (β_2m) in gray in all schematics. (**d**–**f**) CD1d molecule of γδ TCR complex (**d**), type II NKT cell TCR complex (**e**) and type I NKT cell TCR complex (**f**). CDR1α and CDR1δ (labeled 1α and 1δ, respectively), purple; CDR2α (2α) and CDR2δ (2δ), green; CDR3α (3α) and CDR3δ (3δ), yellow; CDR1β (1β) and CDR1γ (1γ), red; CDR2β (2β) and CDR2γ (2γ), blue; CDR3β (3β) and CDR3γ (3γ), orange. Black spheres represent the center of mass of the variable domains of TCRα (V_α) and TCRβ (V_β) chains; A′ and F′ refer to the pockets in CD1d. (**g**–**i**) Structural footprint of the γδ, type II and type I NKT TCRs on the surface of the CD1d–antigen complex. CDR loops are colored accordingly as per **d**, **e** and **f**; the lipid antigen is represented as spheres.

'Lock and key' antigen recognition

Given that TCR plasticity and rigidity is a central theme in T cell–mediated recognition of antigen-presenting molecules[29], we next determined the extent of conformational change upon a γδ TCR recognizing CD1d. Accordingly, with the structures of the binary human CD1d–α-GalCer[30] and nonliganded 9C2 γδ TCR, we addressed the degree of plasticity underpinning γδ TCR recognition of CD1d–α-GalCer. Upon 9C2 γδ TCR complexation, there was essentially no major movement discerned in CD1d or α-GalCer itself (r.m.s. deviation <1.0 Å). Similarly, there was very little movement in the CDR loops of the 9C2 γδ TCR, although the mobile CDR3γ loop in the unligated state became ordered upon CD1d–α-GalCer engagement. Accordingly, a rigid 'lock and key' mechanism underpinned 9C2 γδ TCR recognition of CD1d–α-GalCer.

The interactions with the α-GalCer ligand were mediated exclusively via the CDR3γ loop. In this regard, the mode of γδ TCR–α-GalCer recognition shared some features of XV19 TCR-CD1d-sulfatide recognition, in which only the CDR3β loop interacted with the sulfatide headgroup[17]. Within the 9C2 γδ TCR ternary complex, Arg103γ and Tyr111γ contacted directly the galactose moiety, hydrogen-bonding to the 3′-OH and 4′-OH moieties, thereby indicating that γδ TCR recognition would be impacted by modifications at these sites (**Fig. 6d**). Tyr111γ and the main chain of the CDR3γ loop also formed van der Waals contacts with Trp153, a CD1d residue that packs against the lipid antigen, and represents a key sequence difference between mouse and human CD1d[31], thereby suggesting a rationale as to why the 9C2 γδ TCR does not cross-react with mouse CD1d–α-GalCer. The 6′-OH moiety was situated next to a small cavity between the CD1d α1-helix and the CDR3δ loop, indicating that the 9C2 γδ TCR could tolerate substitutions at this position (**Fig. 6d**). The mode of 9C2 γδ TCR–α-GalCer recognition also suggested that this γδ TCR could potentially interact with β-linked ligands such as sulfatide. In the CD1d–α-GalCer–reactive γδ TCRs we characterized, the CDR3γ loop exhibited marked sequence diversity (**Table 1**), indicating that this hypervariability could potentially fine-tune the specificity to CD1d-restricted ligands. Accordingly, the non–germ line–encoded CDR3γ loop of the 9C2 γδ TCR has a major role in determining specificity for the lipid antigen.

DISCUSSION

Here we provide to our knowledge the first molecular insight into how a γδ TCR can interact with an antigen-presenting molecule in a ligand-dependent manner. γδ TCRs are known to interact with some CD1 molecules, including CD1a, CD1c and CD1d, and in at least some of these examples, lipid antigens appear to be involved[13,14,32], thereby suggesting a potential blurring of the boundaries between the ligands that the αβ T cell and γδ T cell lineages can interact with. Consistent with this, we found that human $V_\delta1^+$ γδ TCRs can directly interact with CD1d bound to α-GalCer, a ligand that is typically associated with type I NKT cells. Given that α-GalCer, and its closely related analogs, are potential therapeutic agents for type I NKT cells[33], it will be important to develop a stronger understanding of the functional capacity of

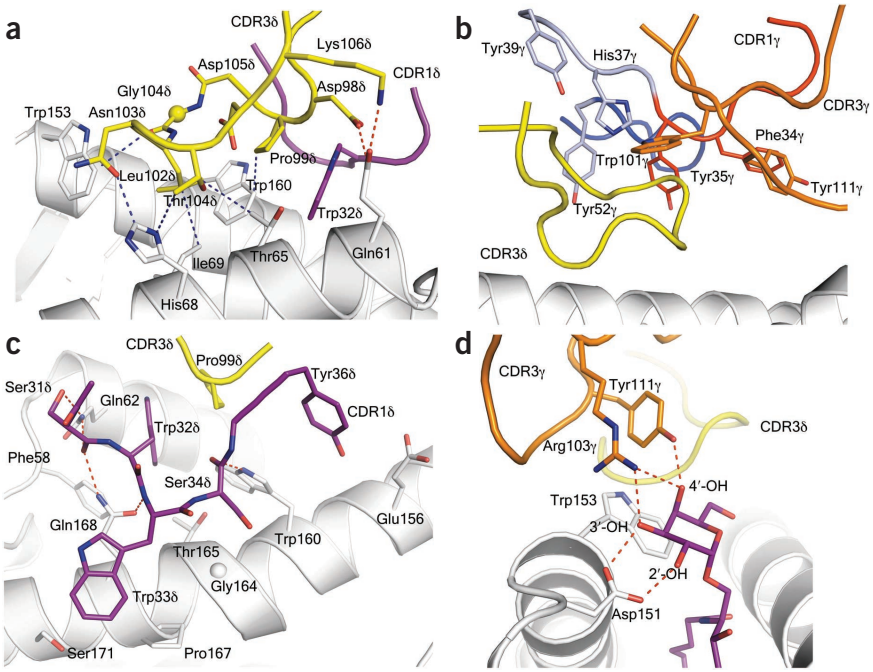

Figure 6 Interactions at the γδ TCR–CD1d–α-GalCer interface. (**a**) Interaction between the CDR3δ (yellow) and the CD1d molecule (white). The CD1d residues interacting with the CDR3δ are in white sticks, the CDR3δ are in yellow sticks. The CDR1δ is represented in purple with Trp32δ in stick format. (**b**) Interaction of the aromatic residues arising from the CDR1γ (red), CDR2γ (blue), framework γ (pale blue) and CDR3γ (orange) surrounding the CDR3δ (yellow). (**c**) Interaction of the CDR1δ (purple) with the CD1d molecule (white), and Pro99δ (partially shown only) in yellow. (**d**) Interaction between the CDR3γ (orange) with α-GalCer (purple sticks), as well as the CDR3δ (yellow). The red dashed lines represent hydrogen bonds and the blue dashed lines represent hydrophobic interactions between the residues in all schematics. Spheres in **a** and **c** represent the C_α atoms of the Gly104 and Gly164 from CD1δ, respectively.

CD1d-dependent γδ T cells in terms of their ability to target and kill tumor cells, and provide help to antigen-presenting cells and other immune cells. Considering a recent report that the gut *Bacteroides* species produce a form of α-GalCer, coupled with the abundance of $V_\delta1^+$ γδ T cells in intestinal tissues, it will be interesting to determine whether these cells have a functional role in this location[34]. Moreover, as most of these CD1d-restricted γδ T cells showed clear autoreactivity against human CD1d, future functional studies should aim to determine whether these cells are sensitive to inflammatory stimuli such as TLR ligands that can modulate self-lipid antigen presentation by CD1d, and cytokines such as IL-12 and IL-18, which can enhance self antigen–mediated stimulation of type I NKT cells[35,36]. The observation that some of these γδ T cells were also reactive to the neuronal tissue self-glycolipid sulfatide presented by CD1d, was reminiscent of another study[14] and suggests a possible role for these cells in multiple sclerosis, an autoimmune disease where enrichment of $V_\delta1^+$ γδ T cells has been observed[37].

We provided insight into how the αβ T cell and γδ T cell lineages can interact with the same antigen-presenting molecule bound to the same ligand. In this regard, the mode of γδ TCR–CD1d–α-GalCer recognition is markedly different from that of type I NKT TCR recognition of CD1d bound to α-linked or β-linked ligands[25,28]. The γδ TCR docked orthogonally over the extreme end of the A′ pocket of CD1d, whereas type I NKT TCRs bind in a parallel manner perched over the F′ pocket[3]. The γδ TCR docking was more analogous, in broad terms, to type II NKT docking onto CD1d-sulfatide[16,17], although the roles of the respective αβ and γδ TCR chains, and associated CDR loops, differed markedly. In the γδ TCR–CD1d–α-GalCer ternary complex, although the CDR3δ loop bound to CD1d, the CDR1δ loop clearly had a dominating role in interacting with CD1d. This CDR1δ loop was characterized by two prominent tryptophan residues, which collectively formed a focused aromatic cluster that engaged CD1d, thereby suggesting that this loop engendered CD1d autoreactivity. This CDR1δ-encoded tryptophan pairing was only found in the gene encoding $V_\delta1$, thereby providing a basis for the biased $V_\delta1$ TCR usage of these CD1d-restricted γδ TCRs. Notably, $V_\delta1^+$ γδ T cells also interact with CD1a and CD1c[32], and three of the CD1d contact residues (Gln62, Ile69 and Thr165) are conserved or conservatively substituted between CD1a and CD1c, suggesting that a common docking mode may potentially underpin $V_\delta1^+$ γδ TCR–CD1 interactions in general.

The CD1d-restricted $V_\delta1^+$ γδ TCRs displayed γ-chain diversity, which was consistent with the 9C2 γδ TCR–CD1d–α-GalCer ternary complex, whereby the γ-chain sat adjacent to the antigen-binding cleft, with the germ line–encoded CDR1γ and CDR2γ loops having a limited or no role in mediating contacts with CD1d. However, the CDR3γ loop underpinned α-GalCer reactivity, with direct interactions being mediated with the galactosyl head group. Moreover, as the CDR3γ loop displayed considerable sequence variation among the CD1d–α-GalCer–restricted γδ TCRs, this loop may potentially alter the threshold of reactivity for α-GalCer or the specificity to other CD1d-restricted ligands.

Our findings show that humans have a diverse repertoire of γδ T cells with the capacity to bind to CD1d that is modulated in an antigen-dependent manner. Moreover, we provided the molecular basis for how a γδ TCR can specifically target an antigen in complex with an antigen-presenting molecule. This sets the stage for additional studies exploring the extent of γδ T cell reactivity to the broad range of lipid antigens presented by various CD1 isoforms in humans. Considering the preferential tissue and mucosal location of $V_\delta1$ γδ T cells, these findings should ultimately shed light on the types of molecules that are targeted by this important and enigmatic component of the immune system.

METHODS

Methods and any associated references are available in the online version of the paper.

Accession codes. Protein Data Bank: 4LFH for the γδ TCR and 4LHU for the γδ TCR–CD1d–α-GalCer complex.

Note: Any Supplementary Information and Source Data files are available in the online version of the paper.

ACKNOWLEDGMENTS

We thank the staff at the MX1 and MX2 beamlines of the Australian Synchrotron for assistance with data collection, M. Sandoval, M. Ciula, D. Littler, R. Berry, J. Waddington, P. Neeson and D. Ritchie for technical assistance, provision of reagents and/or advice, staff from the flow cytometry facilities in the Melbourne Brain Centre and the Department of Microbiology and Immunology at The University

of Melbourne and D. Maksel from the Macromolecular Crystallization Facility at Monash University for technical assistance, P. Savage (Brigham Young University) for providing PBS44 glycolipid, G. Besra (University of Birmingham, UK) and S. Porcelli (Albert Einstein College of Medicine) for providing α-glucosylceramide and the α-GalCer analog OCH, and D. Vignali (St. Jude Children's Research Hospital) and S. Turner (The University of Melbourne) for providing pMIG expression vector. This work was supported by the Australian Research Council and the National Health and Medical Research Council of Australia (NHMRC). N.A.G. is supported by a Leukaemia Foundation of Australia Postgraduate Scholarship; T.B. is supported by a Pfizer Australia Fellowship; S.G. and O.P. are supported by Australian Research Council Future Fellowships; D.G.P. is supported by an NHMRC Peter Doherty Fellowship; J.R. is supported by an NHMRC Australia Fellowship; D.I.G. is supported by an NHMRC Senior Principal Research Fellowship.

AUTHOR CONTRIBUTIONS

A.P.U. identified and performed cellular and molecular characterization of γδ T cells, and produced TCR protein complexes for crystallographic studies. J.L.N., A.P.U. and S.G. solved the crystal structures and performed structural analysis. T.B. undertook SPR investigations. O.P. designed and generated human CD1d-BirA constructs. R.T.L. generated C1R-CD1d transductants. A.P.U., D.G.P., N.A.G., K.G.M. and R.T.L. performed cell-based experiments, including glycolipid specificity and functional studies. J.R. and D.I.G. were joint senior authors: co-led the investigation, devised the project and wrote the manuscript.

COMPETING FINANCIAL INTERESTS

The authors declare no competing financial interests.

1. Godfrey, D.I., Rossjohn, J. & McCluskey, J. The fidelity, occasional promiscuity, and versatility of T cell receptor recognition. *Immunity* **28**, 304–314 (2008).
2. Kjer-Nielsen, L. *et al.* MR1 presents microbial vitamin B metabolites to MAIT cells. *Nature* **491**, 717–723 (2012).
3. Rossjohn, J., Pellicci, D.G., Patel, O., Gapin, L. & Godfrey, D.I. Recognition of CD1d-restricted antigens by natural killer T cells. *Nat. Rev. Immunol.* **12**, 845–857 (2012).
4. Brenner, M.B. *et al.* Identification of a putative second T-cell receptor. *Nature* **322**, 145–149 (1986).
5. Vantourout, P. & Hayday, A. Six-of-the-best: unique contributions of gamma delta T cells to immunology. *Nat. Rev. Immunol.* **13**, 88–100 (2013).
6. Schild, H. *et al.* The nature of major histocompatibility complex recognition by gamma delta T cells. *Cell* **76**, 29–37 (1994).
7. Crowley, M.P. *et al.* A population of murine gammadelta T cells that recognize an inducible MHC class Ib molecule. *Science* **287**, 314–316 (2000).
8. Wingren, C., Crowley, M.P., Degano, M., Chien, Y. & Wilson, I.A. Crystal structure of a gammadelta T cell receptor ligand T22: a truncated MHC-like fold. *Science* **287**, 310–314 (2000).
9. Willcox, C.R. *et al.* Cytomegalovirus and tumor stress surveillance by binding of a human gammadelta T cell antigen receptor to endothelial protein C receptor. *Nat. Immunol.* **13**, 872–879 (2012).
10. Constant, P. *et al.* Stimulation of human gamma delta T cells by nonpeptidic mycobacterial ligands. *Science* **264**, 267–270 (1994).
11. Vavassori, S. *et al.* Butyrophilin 3A1 binds phosphorylated antigens and stimulates human [gamma][delta] T cells. *Nat. Immunol.* **14**, 908–916 (2013).
12. Russano, A.M. *et al.* Recognition of pollen-derived phosphatidyl-ethanolamine by human CD1d-restricted gamma delta T cells. *J. Allergy Clin. Immunol.* **117**, 1178–1184 (2006).
13. Dieude, M. *et al.* Cardiolipin binds to CD1d and stimulates CD1d-restricted gammadelta T cells in the normal murine repertoire. *J. Immunol.* **186**, 4771–4781 (2011).
14. Bai, L. *et al.* The majority of CD1d-sulfatide-specific T cells in human blood use a semiinvariant Vdelta1 TCR. *Eur. J. Immunol.* **42**, 2505–2510 (2012).
15. Godfrey, D.I. & Rossjohn, J. New ways to turn on NKT cells. *J. Exp. Med.* **208**, 1121–1125 (2011).
16. Girardi, E. *et al.* Type II natural killer T cells use features of both innate-like and conventional T cells to recognize sulfatide self antigens. *Nat. Immunol.* **13**, 851–856 (2012).
17. Patel, O. *et al.* Recognition of CD1d-sulfatide mediated by a type II natural killer T cell antigen receptor. *Nat. Immunol.* **13**, 857–863 (2012).
18. Xu, B. *et al.* Crystal structure of a gammadelta T-cell receptor specific for the human MHC class I homolog MICA. *Proc. Natl. Acad. Sci. USA* **108**, 2414–2419 (2011).
19. Allison, T.J., Winter, C.C., Fournie, J.J., Bonneville, M. & Garboczi, D.N. Structure of a human gammadelta T-cell antigen receptor. *Nature* **411**, 820–824 (2001).
20. Li, H. *et al.* Structure of the Vdelta domain of a human gammadelta T-cell antigen receptor. *Nature* **391**, 502–506 (1998).
21. Adams, E.J., Chien, Y.H. & Garcia, K.C. Structure of a gammadelta T cell receptor in complex with the nonclassical MHC T22. *Science* **308**, 227–231 (2005).
22. Adams, E.J., Strop, P., Shin, S., Chien, Y.H. & Garcia, K.C. An autonomous CDR3delta is sufficient for recognition of the nonclassical MHC class I molecules T10 and T22 by gammadelta T cells. *Nat. Immunol.* **9**, 777–784 (2008).
23. Wun, K.S. *et al.* A minimal binding footprint on CD1d-glycolipid is a basis for selection of the unique human NKT TCR. *J. Exp. Med.* **205**, 939–949 (2008).
24. Kjer-Nielsen, L. *et al.* A structural basis for selection and cross-species reactivity of the semi-invariant NKT cell receptor in CD1d/glycolipid recognition. *J. Exp. Med.* **203**, 661–673 (2006).
25. Borg, N.A. *et al.* CD1d-lipid-antigen recognition by the semi-invariant NKT T-cell receptor. *Nature* **448**, 44–49 (2007).
26. Mallevaey, T. *et al.* A molecular basis for NKT cell recognition of CD1d-self-antigen. *Immunity* **34**, 315–326 (2011).
27. Matulis, G. *et al.* Innate-like control of human iNKT cell autoreactivity via the hypervariable CDR3beta loop. *PLoS Biol.* **8**, e1000402 (2010).
28. Pellicci, D.G. *et al.* Recognition of beta-linked self glycolipids mediated by natural killer T cell antigen receptors. *Nat. Immunol.* **12**, 827–833 (2011).
29. Garcia, K.C. *et al.* Structural basis of plasticity in T cell receptor recognition of a self peptide-MHC antigen. *Science* **279**, 1166–1172 (1998).
30. Koch, M. *et al.* The crystal structure of human CD1d with and without alpha-galactosylceramide. *Nat. Immunol.* **6**, 819–826 (2005).
31. Godfrey, D.I., McCluskey, J. & Rossjohn, J. CD1d antigen presentation: treats for NKT cells. *Nat. Immunol.* **6**, 754–756 (2005).
32. Russano, A.M. *et al.* CD1-restricted recognition of exogenous and self-lipid antigens by duodenal gamma delta+ T lymphocytes. *J. Immunol.* **178**, 3620–3626 (2007).
33. Cerundolo, V., Silk, J.D., Masri, S.H. & Salio, M. Harnessing invariant NKT cells in vaccination strategies. *Nat. Rev. Immunol.* **9**, 28–38 (2009).
34. Wieland Brown, L.C. *et al.* Production of alpha-galactosylceramide by a prominent member of the human gut microbiota. *PLoS Biol.* **11**, e1001610 (2013).
35. Brennan, P.J. *et al.* Invariant natural killer T cells recognize lipid self antigen induced by microbial danger signals. *Nat. Immunol.* **12**, 1202–1211 (2011).
36. Brigl, M. *et al.* Innate and cytokine-driven signals, rather than microbial antigens, dominate in natural killer T cell activation during microbial infection. *J. Exp. Med.* **208**, 1163–1177 (2011).
37. Nick, S. *et al.* T cell receptor gamma delta repertoire is skewed in cerebrospinal fluid of multiple sclerosis patients: molecular and functional analyses of antigen-reactive gamma delta clones. *Eur. J. Immunol.* **25**, 355–363 (1995).

ONLINE METHODS

γδ T cell identification and isolation. Healthy human peripheral blood cells were obtained with informed consent from blood donors to the Australian Red Cross Blood Service, with ethics approval from both Red Cross (approval number 11-05VIC-12) and University of Melbourne Human Research and Ethics committee (approval number 1035100). PBMCs were isolated by density gradient centrifugation (Histopaque-1077, Sigma). Cells were stained with antibodies specific for CD3ε (UCHT1, eBioscience and Becton Dickinson), CD4 (RPA-T4, Becton Dickinson), CD8α (SK1, Becton Dickinson), CD19 (HIB19, BioLegend), CD69 (FN50, Becton Dickinson), TCR $V_{\delta}1$ (TS8.2, Thermo Scientific), CD161 (191B8, Miltenyi Biotec), pan–γδ TCR (11F2 and B1, Becton Dickinson), pan–αβ TCR (T10B9.1A-31, Becton Dickinson), $V_{\alpha}24$ (C15, Beckman Coulter), $V_{\beta}11$ (C21, Beckman Coulter), $V_{\alpha}24$-$J_{\alpha}18$ (6B11, BioLegend), 7-aminoactinomycin D viability dye (Sigma) and mouse IgG isotype control (MOPC-21 and X40, Becton Dickinson). All antibodies were used at an empirically determined dilution factor providing optimum signal-to-noise ratio. Human and mouse CD1d tetramers were produced in-house using a baculovirus expression system, similar to that previously described[38]. Lipid antigens were prepared in either Tween-sucrose-histidine buffer (0.5% Tween 20, 57 mg/ml sucrose and 7.5 mg/ml L-histidine) or 0.5% tyloxapol and loaded into CD1d at either a 3:1 or 6:1 lipid:protein molar ratio. α-GalCer was supplied by Alexis Biochemicals or provided by P. Savage (C24:1 PBS44 analog; Brigham Young University). α-GlcCer C20:2 and the α-GalCer analog OCH were provided by G. Besra (University of Birmingham, UK). C12 β-GalCer, C12 β-GlcCer, C24:1 β-GlcCer, disialo-ganglioside GD3, lysophosphatidylethanolamine (LPE) and lysophosphatidylcholine (LPC) were purchased from Avanti Polar Lipids. Cells were analyzed using an LSR Fortessa, LSRII or Canto flow cytometer (BD Biosciences), and data were processed with FlowJo (Tree Star Inc.) software. In some experiments, NKT cells were enriched by human CD1d–α-GalCer tetramer-phycoerythrin staining followed by anti-phycoerythrin–mediated MACS magnetic bead purification (Miltenyi Biotec). After enrichment $CD3^+$ CD1d–α-GalCer $tetramer^+$ NKT cells were further enriched by sorting using a FACSAria (BD Biosciences). Enriched NKT cells were stimulated *in vitro* for 48 h with plate-bound anti-CD3 (UCHT1, 10 μg/ml), soluble anti-CD28 (CD28.2, 10 μg/ml), phytohemagglutinin (0.5 μg/ml), recombinant human IL-2 (100 U/ml, PeproTech) and IL-7 (50 ng/ml, eBioscience), followed by maintenance with IL-2 and IL-7 for 14–21 d. Cells were cultured in complete medium consisting of a 50:50 (v/v) mixture of RPMI-1640 and AIM-V (Invitrogen) supplemented with 10% (v/v) FCS (JRH Biosciences), penicillin (100 U/ml), streptomycin (100 μg/ml), Glutamax (2 mM), sodium pyruvate (1 mM), nonessential amino acids (0.1 mM) and HEPES buffer (15 mM), pH 7.2–7.5 (all from Invitrogen Life Technologies), plus 50 μM 2-mercaptoethanol (Sigma-Aldrich). For stimulation assays, $CD3^+$ γδ TCR^+ $V_{\delta}1^+$ CD1d–α-GalCer-$tetramer^+$ or $CD3^+$ αβ TCR^+ $V_{\delta}1^-$ CD1d–α-GalCer-$tetramer^+$ (type I NKT) were cultured for 16 h with PMA (10 ng/ml) and ionomycin (1 μg/ml). Culture supernatants were analyzed for cytokines with a cytometric bead array human flex set (BD Biosciences).

Single-cell PCR. cDNA from sorted CD1d–α-GalCer $tetramer^+$ γδ TCR^+ cells was generated by the addition of 2 μl per well of buffer containing SuperScript VILO (Invitrogen) and 0.1% Triton X-100 (Sigma), and incubated according to manufacturer's instructions. Transcripts encoding $V_{\delta}1$ and V_{γ} were amplified by two rounds of semi-nested PCR[39] using primers listed in **Supplementary Table 3** and PCR master mix (Promega). PCR products were separated on a 1.5% agarose gel and sequenced (Applied Genetics Diagnostics, University of Melbourne).

Generation of cell lines. T cell lines expressing γδ TCR and αβ TCR were generated by cloning full-length genes encoding γ- and δ- or α- and β-chains separated by a hydrolase element P2A linker into the pMIGII expression vector[40]. Parental Jurkat-76 cells were transduced with vectors encoding 9C2 (TCR $V_{\gamma}5$-$V_{\delta}1$ with CDR3 sequences from **Table 1**, sequence 5) or control HLA peptide–specific TCR, or SKW3 cells were transduced a vector encoding NKT15 (TCR $V_{\alpha}24$-$J_{\alpha}18$-$V_{\beta}11$-$J_{\beta}2.7$; ref. 24). Jurkat-76 cells and SKW3 cells were provided by L. Kjer-Nielsen (University of Melbourne). These have not been recently authenticated or tested for *Mycoplasma*. Parental Jurkat-76 cells and SKW3 cells lack endogenous TCR α-chains and β-chains[41,42], and therefore TCR specificity is conferred by the transgene. For antigen-presenting cell lines, parental C1R cells were transduced with human CD1d heavy chain using a pMIGII expression vector. After transduction, $CD1d^{int}$ and $CD1d^{hi}$ cells were purified by sorting and maintained as separate cell lines. For coculture assays, Jurkat-76 T cells lines were cultured with or without C1R cells expressing intermediate or high levels of CD1d (3×10^4 of each cell line) for 6–12 h in round-bottom 96-well plates.

Cloning and expression of genes encoding γδ TCR and human CD1d. Paired sequences encoding TCR-γ and TCR-δ sequences from a single cell (**Table 1**, sequence 5) were used to clone a construct encoding the ectodomain of γδ TCR with a C-terminal thrombin cleavage site, leucine zippers and His tag (**Supplementary Fig. 2a**) into the expression vector pHLsec. 9C2 γδ TCR was expressed by transient transfection of mammalian HEK-293S.GnTI cells[43]. Protein was purified from culture supernatant using immobilized metal affinity chromatography and gel filtration. Leucine zippers and N-linked glycosylation were removed by digests with thrombin (Sigma) and endoglycosidase H (New England Biolabs), respectively. Soluble NKT15 type I NKT TCR and human CD1d for crystallography were produced as previously described[24]. For CD1d tetramer production and SPR, human CD1d extracellular domain was designed with a C-terminal BirA tag and a 6×His tag (amino acid sequence at the C terminus: GSGLNDIFEAQKIEWHEHHHHHH). A codon-optimized version of the gene encoding human CD1d-BirA (GenScript) was subcloned into pFastBacDual vector (Invitrogen) with restriction sites XmaI and KpnI, along with human beta-2-microglobulin, as described previously[24]. Expression, purification and biotinylation of human CD1d-BirA construct was carried out as described previously[24].

Surface plasmon resonance. SPR experiments were conducted at 25 °C on a BIAcore 3000 instrument using 10 mM HEPES-HCl (pH 7.4) and 300 mM NaCl. The biotinlyated CD1d complexes were immobilized to a SA-Chip (GE) with a surface density of ~1,000 response units. Twofold dilutions of 9C2 γδ TCR or type I NKT TCR were injected over the captured CD1d at 10 μl/min. The final response was calculated by subtracting the response of a blank flow cell (streptavidin alone) and buffer alone from the TCR-CD1d complex. The equilibrium data were analyzed using GraphPad Prism.

Crystallization, structure determination and refinement. Tetragonal crystals of the deglycosylated 9C2 γδ TCR grew in 40% PEG 300, 0.1 M Na-cacodylate and 0.2 M Ca-acetate. Crystals were flash-frozen, and data were collected at the Australian Synchrotron MX1 facility, Melbourne. Data were processed with the program XDS[44] and were scaled with the SCALA program of the CCP4 suite. TCR crystals belonged to the $P4_22_12$ space group and diffracted to 2.3 Å resolution. Molecular replacement was carried out with the program PHASER[45], using the structures of the human γδ TCR δ1A/B-3 (for the δ-chain) and the G115 $V_{\gamma}9$-$V_{\delta}2^+$ TCR (for the γ-chain and C_{δ}) (PDB codes 3OMZ and 1HXM, respectively[18,19]) as separate search ensembles. An initial run of rigid body refinement was performed with the refinement program BUSTER (G. Bricogne *et al.* BUSTER version 2.10 Cambridge, United Kingdom: Global Phasing Ltd.; 2011) and the CDR loops of the TCR were subsequently rebuilt using the program COOT[46]. BUSTER was then used for the subsequent refinement cycles to lead to a final model with R_{fac} and R_{free} values of 18.9% and 24.1%, respectively. The complex crystals were obtained in 8–12% PEG 8000, 0.1–0.2 mM $MgCl_2$ and 0.1 M Tris-HCl 7.0 using a mixture of the γδ TCR (glycosylated form) and CD1d–α-GalCer (C24:1, PBS44 analog) in a 1:1 molar ratio. Crystals were flash-frozen using 20% glycerol solution as cryoprotectant. Data were collected at the MX2 beamline (Australian Synchrotron) and were processed with XDS software and were scaled with the SCALA program of the CCP4 suite to 2.87 Å. The crystal belonged to the $C222_1$ space group, and the unit cell is consistent with one complex in the asymmetric unit. A molecular replacement solution was found with the program PHASER using the structure of human CD1d without any lipid (PDB code 2PO6; ref. 25) and the unligated γδ TCR as two separate search ensembles. The model was then refined into the experimental map before iterative model building with COOT and refinement with BUSTER with a final R_{fac} and R_{free} values of 20.6% and 24.3%, respectively. The density of the α-GalCer headgroup was unambiguous and the electron density

doi:10.1038/ni.2713

at the interface was clear. The quality of all structures was confirmed at the Research Collaboratory for Structural Bioinformatics Protein Data Bank Data Validation and Deposition Services website. All presentations of molecular graphics were created with the PyMOL molecular visualization system (The PyMOL Molecular Graphics System, Version 1.5.0.4 Schrödinger, LLC.).

The surface electrostatic potential map was calculated using the nonlinear mode of the adaptive Poisson-Boltzmann solver (APBS)[47,48].

38. Matsuda, J.L. *et al.* Tracking the response of natural killer T cells to a glycolipid antigen using CD1d tetramers. *J. Exp. Med.* **192**, 741–754 (2000).
39. Kedzierska, K., Turner, S.J. & Doherty, P.C. Conserved T cell receptor usage in primary and recall responses to an immunodominant influenza virus nucleoprotein epitope. *Proc. Natl. Acad. Sci. USA* **101**, 4942–4947 (2004).
40. Szymczak, A.L. *et al.* Correction of multi-gene deficiency *in vivo* using a single 'self-cleaving' 2A peptide-based retroviral vector. *Nat. Biotechnol.* **22**, 589–594 (2004).
41. Heemskerk, M.H. *et al.* Redirection of antileukemic reactivity of peripheral T lymphocytes using gene transfer of minor histocompatibility antigen HA-2-specific T-cell receptor complexes expressing a conserved alpha joining region. *Blood* **102**, 3530–3540 (2003).
42. Shima, E.A. *et al.* Gene encoding the alpha chain of the T-cell receptor is moved immediately downstream of c-myc in a chromosomal 8;14 translocation in a cell line from a human T-cell leukemia. *Proc. Natl. Acad. Sci. USA* **83**, 3439–3443 (1986).
43. Aricescu, A.R., Lu, W. & Jones, E.Y. A time- and cost-efficient system for high-level protein production in mammalian cells. *Acta Crystallogr. D Biol. Crystallogr.* **62**, 1243–1250 (2006).
44. Kabsch, W. XDS. *Acta Crystallogr. D Biol. Crystallogr.* **66**, 125–132 (2010).
45. McCoy, A.J. Solving structures of protein complexes by molecular replacement with Phaser. *Acta Crystallogr. D Biol. Crystallogr.* **63**, 32–41 (2007).
46. Emsley, P., Lohkamp, B., Scott, W.G. & Cowtan, K. Features and development of Coot. *Acta Crystallogr. D Biol. Crystallogr.* **66**, 486–501 (2010).
47. Baker, N.A., Sept, D., Joseph, S., Holst, M.J. & McCammon, J.A. Electrostatics of nanosystems: application to microtubules and the ribosome. *Proc. Natl. Acad. Sci. USA* **98**, 10037–10041 (2001).
48. Holst, M., Baker, N.A. & Wang, F. Adaptive multilevel finite element solution of the Poisson-Boltzmann equation I. Algorithms and examples. *J. Comput. Chem.* **21**, 1319–1342 (2000).